Published in final edited form as:
Dev Cell. 2014 March 10; 28(5): 520–533. doi:10.1016/j.devcel.2014.02.001.

Release from myosin V via regulated recruitment of an E3 Ub ligase controls organelle localization

Richard G. Yau[1], **Yutian Peng**[2], **Rajeshwari R. Valiathan**[2], **Shanda R. Birkeland**[4], **Thomas E. Wilson**[1,4,5], and **Lois S. Weisman**[1,2,3]

[1]Program in Cell and Molecular Biology, University of Michigan Medical School, Ann Arbor MI 48109, USA

[2]Life Sciences Institute, University of Michigan, Ann Arbor, MI 48109, USA

[3]Department of Cell and Developmental Biology, University of Michigan Medical School, Ann Arbor MI 48109, USA

[4]Department of Pathology, University of Michigan Medical School, Ann Arbor MI 48109, USA

[5]Department of Human Genetics, University of Michigan Medical School, Ann Arbor MI 48109, USA.

Summary

Molecular motors transport organelles to specific subcellular locations. Upon arrival at their correct locations, motors release organelles via unknown mechanisms. The yeast myosin-V, Myo2, binds the vacuole specific adaptor, Vac17, to transport the vacuole from the mother cell to the bud. Here, we show that vacuole detachment from Myo2 occurs in multiple regulated steps along the entire pathway of vacuole transport. Detachment initiates in the mother cell with the phosphorylation of Vac17 which recruits the E3 ligase, Dma1, to the vacuole. However, Dma1 recruitment also requires the assembly of the vacuole transport complex and is first observed after the vacuole enters the bud. Dma1 remains on the vacuole until the bud and mother vacuoles separate. Subsequently, Dma1 targets Vac17 for proteasomal degradation. Notably, we find that the termination of peroxisome transport also requires Dma1. We predict that this is a general mechanism which detaches myosin-V from select cargoes.

Introduction

Proper subcellular localization of organelles is essential for cell function. Actin based myosin V motors, conserved across eukaryotes, transport many organelles to their correct subcellular locations. Myosin V attaches to cargoes and initiates transport via the interaction

Address correspondence to: Lois S. Weisman Life Sciences Institute 210 Washtenaw Ave., Rm 6437 The University of Michigan Ann Arbor, MI 48109-2216, USA Tel: 734.647.2537 Fax: 734.615.5493 lweisman@umich.edu.

of the myosin V cargo binding domain with cargo specific adaptor proteins. Upon arrival at their destinations, cargoes are released from myosin V which terminates transport and deposits cargoes at their correct subcellular locations. How molecular motors release cargoes is poorly understood.

Studies in *Saccharomyces cerevisiae* have provided significant insights into the mechanisms that regulate myosin V. The yeast myosin V motor, Myo2, transports most of the cytoplasmic organelles from the mother cell to the bud. Myo2 attaches to cargoes via direct interactions with multiple cargo specific adaptors which enable Myo2 to selectively transport subsets of cargoes to different locations at distinct times. For example, Mmr1, Ypt11(Eves et al., 2012; Fortsch et al., 2011; Itoh et al., 2004; Itoh et al., 2002), Inp2 (Fagarasanu et al., 2006), Ypt31/32, Sec4, Sec15 (Jin et al., 2011; Lipatova et al., 2008; Santiago-Tirado et al., 2011), Kar9 (Korinek et al., 2000) and Vac17 (Ishikawa et al., 2003; Tang et al., 2003) attach Myo2 to mitochondria, peroxisomes, secretory vesicles, astral microtubules and the vacuole respectively.

Studies of vacuole transport have revealed that cargo adaptors play key roles in both the spatial and temporal regulation of myosin V based transport. Early in the cell cycle, the vacuole specific adaptor, Vac17, is phosphorylated by the cyclin dependent kinase, Cdk1. Cdk1 phosphorylation promotes the interaction between Vac17 and Myo2 thereby attaching Myo2 to the vacuole (Peng and Weisman, 2008). Myo2 moves a portion of the vacuole from the mother to the bud. Initially, the vacuole in the bud remains connected to the original vacuole in the mother via a segregation structure (Weisman and Wickner, 1988). Eventually, resolution of the segregation structure separates the bud and mother vacuoles (Bartholomew and Hardy, 2009). After vacuole movement terminates, Myo2 continues to transport secretory vesicles to the mother-bud neck (Karpova et al., 2000; Lillie and Brown, 1994). Thus, Myo2 but not the bud vacuole moves to the mother-bud neck. Proper detachment of the vacuole from Myo2 requires the Vac17 PEST sequence. PEST sequences target proteins for rapid degradation. Deletion of the PEST sequence causes an accumulation of Vac17. Interestingly, in the *vac17-ΔPEST* mutant, the vacuole fails to detach from Myo2 and the vacuole is inappropriately transported to the mother-bud neck late in the cell cycle, the site where Myo2 delivers secretory vesicles (Tang et al., 2003).

Here, we present the unexpected finding that the regulated recruitment of an E3 ubiquitin ligase, Dma1, to the vacuole is critical for the accurate detachment of the vacuole from Myo2. In *S. cerevisiae*, Dma1 and its paralogue, Dma2, are known spindle positioning checkpoint proteins. In addition, they play roles in septin ring deposition, spindle positioning and cytokinesis (Fraschini et al., 2004). Dma1 and Dma2 each contain a Forkhead Associated (FHA) domain and a RING domain. FHA domains bind phospho-threonine residues and often exhibit a strong preference for specific residues at the +3 position of the phospho-threonine. For example, the protein Rad53 contains two FHA domains, one recognizes a pTxxI/L motif while the second recognizes a pTxxD motif *in vitro* (Bieganowski et al., 2004; Durocher et al., 1999; Durocher et al., 2000). The RING finger domain of Dma1 and Dma2 is required for E3 ubiquitin ligase activity. Both FHA and RING domains are required for the known roles of Dma1 and Dma2 (Guertin et al., 2002; Johnson and Gould, 2011).

Here, we demonstrate that the detachment of cargoes from myosin V occurs via a Dma1/Dma2 dependent mechanism. For the vacuole, detachment from Myo2 requires the phosphorylation of Vac17-Thr240. This phosphorylation step occurs in the mother cell, the site where Myo2 attaches to the vacuole. Dma1 directly binds phospho-Thr240 and through this interaction, Dma1 localizes to the Myo2/Vac17 transport complex on the vacuole. Intriguingly, recruitment of Dma1 of to the vacuole is dependent on the attachment of Myo2 to the vacuole. Moreover, Dma1 is not observed on the vacuole until the vacuole enters the bud. After recruitment, Dma1 persists on the bud vacuole until after the bud vacuole separates from the mother vacuole. Subsequently, Dma1 targets Vac17 for degradation via the ubiquitin proteasome system (UPS) which releases the bud vacuole from Myo2. Thus, Vac17 phosphorylation, attachment of Myo2 to the vacuole and resolution of the segregation structure each provide different signals recognized by Dma1 which in turn detaches the vacuole from myosin V. Notably, we show that the termination of Myo2 dependent peroxisome transport also requires Dma1/Dma2. Studies on how the vacuole detaches from Myo2 will likely provide insights that are applicable to the termination of the transport of other myosin V cargoes.

Results

An E3 ubiquitin ligase, Dma1, is critical for Vac17 degradation and the termination of vacuole transport

To identify factors required for the detachment of the vacuole from Myo2, we performed a genetic screen. Given that the termination of vacuole movement requires Vac17 turnover (Tang et al., 2003), we sought mutants with elevated Vac17 levels. Wild-type cells transformed with a plasmid encoding *VAC17*-GFP were subjected to EMS mutagenesis and mutants with elevated GFP fluorescence were enriched via Fluorescence Activated Cell Sorting. We obtained mutants that were defective in both the initiation and termination of vacuole transport, as both types of mutants will cause an elevation of Vac17 levels (Tang et al., 2003). Mutants defective in the initiation of vacuole transport were not pursued. One mutant of interest, *vac22-1*, had elevated levels of both Vac17-GFP and endogenous Vac17 (Figure S1A). This indicated that the causative mutation was in a gene related to the turnover of Vac17 rather than a mutation in Vac17-GFP. In *vac22-1*, Vac17-GFP and the vacuole were mis-targeted to the mother-bud neck in large budded cells; the site where Myo2 delivers secretory vesicles late in the cell cycle (Figure S1B). This suggests that the *vac22-1* mutant is defective in the dissociation of Vac17 and the vacuole from Myo2 which causes the vacuole to be inappropriately dragged along the entire Myo2 itinerary.

To identify the causative mutation of the *vac22-1* phenotype, whole genome sequencing was performed for *vac22-1* and the isogenic parental strain. The haploid *vac22-1* mutant was backcrossed with the isogenic wild-type strain. After 3 backcrosses, 12 spores with the *vac22-1* phenotype (elevated Vac17 levels) were pooled together and 12 spores with the wild-type phenotype (normal Vac17 levels) were pooled. Most of the potentially thousands of non-causative EMS induced mutations should randomly distribute between the mutant and wild-type pools. DNA sequenced from the mutant pool was compared to the wild-type pool (Birkeland et al., 2010). The point mutation, *dma1-G232R*, was present only in the

mutant pool. Gly232 is within the FHA domain of Dma1. The equivalent residue of the mammalian Rnf8 FHA domain is located at a turn on the opposite side of the phospho-Thr binding region (Pennell et al., 2010). Thus, Gly232 likely does not contact phospho-Thr and the G232R mutation may disrupt the overall structure of the Dma1 FHA domain.

To determine if *DMA1* is required for the termination of vacuole movement, we generated a *dma1*Δ mutant. We assessed the location of the vacuole in large budded cells, where Myo2 is predicted to localize to the mother-bud neck. In the *dma1*Δ mutant, 40.0±0.5% of large budded cells have vacuoles mis-targeted to the mother-bud neck. That the inappropriate accumulation of vacuoles at the mother-bud neck did not exceed 40% is likely due to the fact that in a percentage of large budded cells the actin cytoskeleton has yet to be re-organized and Myo2 has not yet moved to the mother-bud neck (Pruyne et al., 2004). The presence of vacuoles at the mother-bud neck in wild-type cells was much lower; approximately 10% of large budded cells have this phenotype (Figures 1A and 1B). Furthermore, in the *dma1*Δ mutant, the vacuole colocalized with Vac17-GFP and Myo2-Venus at the mother-bud neck (Figures 1C and 1D). These results suggest that Dma1 is required for the detachment of Vac17 and the vacuole from Myo2.

Notably, expression of *DMA1* but not *dma1-G232R* restores the termination of vacuole movement in the *dma1*Δ mutant (Figures 1A and 1B) and in the *vac22-1* mutant (data not shown). Furthermore, expression of *DMA1* but not *dma1-G232R* rescued Vac17 levels in the *dma1*Δ mutant (Figure 1E) and in the *vac22-1* mutant (data not shown). Therefore, *dma1-G232R* is a null allele and the causative mutation of the *vac22-1* phenotype.

Dma2, the paralogue of Dma1 in *S. cerevisiae*, shares 58% amino acid identity with Dma1 and performs redundant functions in the spindle positioning checkpoint and cytokinesis (Fraschini et al., 2004). To test whether Dma2 also functions in the termination of vacuole movement, the *dma2*Δ and *dma1*Δ *dma2*Δ mutants were generated. In the *dma2*Δ mutant, there was a modest phenotype, 17.3±3.67% of large budded cells accumulate vacuoles at the mother bud neck compared to the *dma1*Δ mutant at 41.6±3.32%. In the *dma1*Δ *dma2*Δ double mutant the phenotype was stronger (71.9±5.90%). In wild-type cells, only 10.5±1.04% of large budded cells show this phenotype (Figures S1C and S1D). These results suggest that Dma2 also functions in the termination of vacuole movement.

We tested whether Dma1 and Dma2 are required for the termination of the transport of peroxisomes, another Myo2 cargo. We chose peroxisomes because their transport is entirely Myo2 dependent and similar to the vacuole, the peroxisome remains intact after transport (Fagarasanu et al., 2006). To visualize peroxisomes, we tagged GFP with the peroxisome targeting sequence, SKL. In wild type cells, peroxisomes were distributed along the periphery of the bud with only 2.1±1.4% of large budded cells showing accumulation of peroxisomes at the mother-bud neck. In the *dma1*Δ*dma2*Δ mutant, peroxisomes were mis-targeted to the mother-bud neck in 56.1±2.2% of large budded cells. This phenotype closely parallels the accumulation of vacuoles at the mother-bud neck in the *dma1*Δ*dma2*Δ mutant (Figure 1F). These results suggest Dma1 and Dma2 function with Myo2 to release at least two types of cargoes. Thus, mechanistic insights gained from studies of Dma1/Dma2 are

likely to be applicable to other myosin V cargoes. To further investigate the mechanisms by which Dma1 and Dma2 regulate cargo release, we focused on the vacuole.

Dma1 localizes to the bud vacuole

Dma1 functions as a spindle checkpoint protein in *Schizosaccharomyces pombe* (Murone and Simanis, 1996). In *S. pombe*, Dma1 localizes to the cytokinetic ring and the spindle pole bodies (SPBs), however, its localization in *S. cerevisiae* was unknown(Guertin et al., 2002). We found that in *S. cerevisiae*, Dma1-GFP localized to regions consistent with the septin ring and the SPBs (Figure 2A) and colocalized with Spc42-mRFP (Figure 2B), a core component of the SPB. Dma1 localizes to the SPBs and septin ring only in large budded cells late in the cell cycle. That Dma1 functions in the termination of vacuole transport prompted us to examine its localization during vacuole inheritance. Early in the cell cycle, Dma1-GFP localized to the vacuole in the bud (Figure 2C) and did not colocalize with Spc42-mRFP, which remained in the mother cell (Figure 2D).

To further determine the timing of Dma1 localization to the vacuole, *DMA1* was tagged with 3xGFP at its endogenous locus. Dma1-3xGFP localization was assessed during vacuole inheritance, from prior to the initiation of vacuole transport until the resolution of the segregation structure. In unbudded and small budded cells where the vacuole has not moved into the bud, no significant localization of Dma1-3xGFP to the vacuole was observed. Dma1-3xGFP was first observed on the portion of the vacuole that crossed the mother-bud neck into the bud. At this time, the vacuole in the bud is connected to the mother vacuole via a segregation structure. Intriguingly, after Dma1 was recruited to the vacuole, the termination of vacuole transport did not immediately occur. Instead, Dma1-3xGFP moved with the vacuole to the bud tip and remained on the vacuole as the bud grew. Dma1-3xGFP persisted on the vacuole at the bud tip until after the segregation structure was resolved and the bud vacuole separated from the mother vacuole (Figures 2E and 2F). These results suggest that both recruitment of Dma1 to the vacuole and Dma1 activity are coordinated with vacuole inheritance.

To determine whether recruitment of Dma1 to the vacuole is dependent on Myo2, we analyzed Dma1-GFP localization in a *myo2-D1297N* mutant. *myo2-D1297N* does not bind Vac17 and the vacuole is not transported to the bud (Eves et al., 2012; Ishikawa et al., 2003). Dma1-GFP failed to accumulate on the vacuole in the *myo2-D1297N* mutant in all small budded cells analyzed. In cells expressing *MYO2*, Dma1-GFP accumulated on the bud vacuole in 76.4±5.7% of small budded cells (Figures 2G and 2H). These results suggest that Dma1 recruitment to the vacuole requires the assembly of the Myo2/Vac17/Vac8 complex. Interestingly, in the *myo2-D1297N* mutant, where Dma1 is not recruited to the vacuole, Vac17 is not degraded (Figure S2). This suggests that the regulated recruitment of Dma1 to the vacuole is critical for Vac17 degradation.

Vac17 residue Thr240 is required for Vac17 degradation and the termination of vacuole transport

The Vac17 PEST sequence is required for the termination of vacuole transport (Tang et al., 2003) (Figure 3A). Notably, T_{240}IIL resides within the PEST sequence and fits the TxxI/L

motif, suggesting that Thr240 may be the binding site on Vac17 for Dma1. To determine whether Thr240 is required for the termination of vacuole transport we generated and characterized the *vac17-T240A* point mutant. The T240A mutation caused an elevation of Vac17 levels (Figure 3B). Furthermore, *vac17-T240A*-GFP and the vacuole accumulated at the mother-bud neck in large budded cells. This contrasts with cells expressing wild-type *VAC17*-GFP, where no GFP signal was detected, consistent with the proper degradation of Vac17-GFP and detachment of the vacuole from Myo2 (Figure 3C). Moreover, in cells expressing *vac17-T240A*, at the mother-bud neck, the vacuole colocalized with Myo2-Venus and *vac17-T240A*-GFP colocalized with mCherry-Myo2 (Figures S3A and S3B). Together, these results suggest that Vac17-Thr240 is required for Vac17 degradation and the regulated detachment of Vac17 and the vacuole from Myo2.

PEST sequences contain serines and threonines that are often phosphorylation sites critical for targeting the protein for degradation (Marchal et al., 1998; Martinez et al., 2003). To determine whether Thr240 was the only potential phosphorylation site in the PEST sequence required for the termination of vacuole transport, we mutated all serines and threonines within the PEST sequence to alanines. We found that in addition to *vac17-T240A*, the point mutant *vac17-S222A* also caused an elevation of Vac17 levels (Figure 3B). Furthermore, *vac17-S222A*-GFP and the vacuole accumulated at the mother-bud neck in large budded cells (Figure 3C). In the *vac17-S222A* mutant, at the mother-bud neck, the vacuole colocalized with Myo2-Venus and *vac17-S222A*-GFP colocalized with Myo2-mCherry (Figures S3A and S3B). These results suggest that, in addition to Vac17-Th240, Vac17-Ser222 is also required for Vac17 degradation and the detachment of Vac17 and the vacuole from Myo2.

Dma1 binds directly to Vac17 at phosphorylated Thr240 *in vitro*

Vac17- $T_{240}III_{243}$ matches the TxxI/L motif recognized by some FHA domains. This raised the intriguing hypothesis that Vac17-Thr240 is the binding site for Dma1. Because FHA domains strictly recognize phospho-threonines, we tested whether Vac17-Thr240 is phosphorylated.

We generated antibodies against a peptide with a central phosphorylated Thr240. To analyze Vac17 phosphorylation, we immunoprecipitated Vac17-GFP expressed in a *vac17*Δ mutant using anti-GFP antibodies. However, we failed to detect Vac17-GFP via western blot or immunoprecipitation (IP) (Figure 4A). In wild-type cells, Vac17 levels are exceedingly low, present at ~20 molecules per cell (Ghaemmaghami et al., 2003; Tang et al., 2006). Thus, detecting phosphorylated Vac17 proved difficult. However, we postulated that Dma1/Dma2 target Vac17 for degradation by binding phosphorylated Thr240. Deletion of *DMA1* and *DMA2* would likely result in the accumulation of phosphorylated forms of Vac17 (Figure 4B). Indeed, Vac17-GFP is stabilized in the *dma1*Δ *dma2*Δ *vac17*Δ mutant. Moreover, Vac17-GFP was recognized by the anti-phosphoThr240 antibody. In contrast, the levels of *vac17-T240A*-GFP are similar when expressed in both the *vac17*Δ and *dma1*Δ *dma2*Δ *vac17*Δ mutants, but was not recognized by the anti-phosphoThr240 antibody, verifying the specificity of this antibody for Thr240.

To determine whether this antibody was phospho-specific, Vac17-GFP was immunoprecipitated from the *dma1*Δ *dma2*Δ *vac17*Δ mutant and treated with λ-phosphatase. Vac17-GFP was dephosphorylated, as indicated by an increase in its electrophoretic mobility, in samples treated with λ-phosphatase but not with the addition of phosphatase inhibitors or in untreated samples (Figure 4C). The anti-phosphoThr240 antibody failed to recognize dephosphorylated Vac17-GFP indicating that this antibody is specific for phospho-Thr240 and that Thr240 is phosphorylated *in vivo*. These results strongly suggest that Vac17-Thr240 is a binding site for Dma1. Moreover, given that *vac17-T240A-GFP* levels were similar in the absence and presence of *DMA1/DMA2* suggests that Thr240 and Dma1/Dma2 function in the same step of the pathway.

To test whether Dma1 binds phosphorylated Vac17-Thr240, *in vitro* binding studies were performed. Recombinant GST-Dma1 or the GST tag alone were immobilized on glutathione beads and incubated with yeast cell extracts from a *dma1*Δ *dma2*Δ *VAC17-TAP* strain where phosphorylated Vac17 accumulates. GST-Dma1 but not the GST tag alone bound Vac17-TAP. However, GST-Dma1 did not bind *vac17-T240A*-TAP. As a control, we show that the Myo2 cargo binding domain, a known Vac17 binding partner, bound the *vac17-T240A*-TAP mutant (Figure 4D). This suggests that the T240A mutation does not affect the overall structure of Vac17 and that Thr240 is required for Dma1 to bind Vac17.

To test whether Dma1 binds phosphorylated Thr240, we performed competition experiments comparing the ability of phosphorylated and unphosphorylated peptides to compete with full-length Vac17 for access to Dma1. Prior to incubation with yeast cell extracts, immobilized GST-Dma1 was first incubated with peptides that contained a central phospho-Thr240, unphosphorylated Thr240 or phospho-Ser222. Addition of the phospho-Thr240 peptide blocked GST-Dma1 from binding Vac17-TAP from cell lysates. In contrast, addition of the unphosphorylated Thr240 or phospho-Ser222 peptides did not affect GST-Dma1 binding to Vac17-TAP (Figure 4E).

To further determine whether Dma1 binds directly to phospho-Thr240, we tested the effect of a peptide with a central phospho-Thr240 on the thermostability of recombinant GST-Dma1 via ThermoFluor. ThermoFluor measures the incorporation of the fluorescent dye, ANS, into proteins undergoing temperature based unfolding. An interaction between GST-Dma1 and its binding partner would potentially stabilize GSTDma1 and cause an increase in its melting temperature (T_m). The T_m of GST-Dma1 alone or with an unphosphorylated peptide was 32.02±0.08 °C and 31.27±0.08 °C, respectively. With a phospho-Thr240 peptide, the T_m of GST-Dma1 was elevated by ~14 °C to 45.60±0.03 °C. To ensure that we were measuring the unfolding of Dma1 and not the GST tag, we measured the thermostability of the GST tag alone. The T_m of GST was 56.24±0.06 °C. The phospho-Thr240 peptide or unphosphorylated peptide had only a minor effect on the T_m of GST which was 57.22±0.05 °C and 57.40±0.01 °C respectively (Figure 4F). Thus, Dma1 directly binds Vac17 at phosphorylated Thr240. Furthermore, these results suggest that Dma1 does not bind Vac17-Ser222. Consistent with this hypothesis, we found that recombinant GST-Dma1 bound *vac17-S222A*-TAP *in vitro* (Figure S4A).

Vac17-pT_{240}IIL_{243} matches the pTxxI/L FHA domain binding motif identified *in vitro*. To determine whether Leu243 was required for the termination of vacuole transport *in vivo*, we generated the *vac17-L243N* mutant. However, expression of *vac17-L243N* in the *vac17*Δ mutant did not cause a defect in the termination of vacuole transport (Figure S4B). We found that 5.6±1.9% of large budded cells expressing *vac17-L243N* had vacuoles at the mother-bud neck. This was similar to 5.6±1.0% of wild-type cells and 3.8±0.8% of cells expressing wild-type *VAC17* (Figure S4C). This suggests that *in vivo*, the *S. cerevisiae* Dma1 FHA domain has some flexibility in the recognition of the residue at the +3 position.

Recruitment of Dma1 to the vacuole requires the interaction between Dma1 and phosphorylated Vac17-Thr240

To test whether Vac17-Thr240 is required for the recruitment of Dma1 to the vacuole, we analyzed the localization of Dma1-GFP in cells expressing *VAC17* or *vac17-T240A*. In cells expressing *VAC17*, Dma1-GFP localized to the vacuole in 82.9±4.3% of small budded cells. In contrast, Dma1-GFP localized to the vacuole in 19.5±1.9% of small budded cells expressing *vac17-T240A* (Figures 5A and 5B). Similarly, Dma1-tdTomato colocalized with Vac17-GFP in 79.8±2.4% of small budded cells and with *vac17-T240A*GFP in 33.6±5.3% of small budded cells (Figure 5C and 5D).

Given that FHA domains bind phospho-Thr, we tested whether the FHA domain of Dma1 is required for Dma1 recruitment to Vac17. We generated the *dma1-R193E* mutant, which contains a charge reversal of a conserved residue in FHA domains that directly contacts phospho-Thr (Durocher et al., 2000). While Dma1-GFP localized to the vacuole in 75.4±4.4% of small budded cells, *dma1-R193E*-GFP failed to localize to the vacuole in all cells analyzed (Figure S5). These results suggest that the interaction between the Dma1 FHA domain and phosphorylated Vac17-Thr240 is critical to recruit Dma1 to the vacuole.

Dma1 is first observed on the vacuole in the bud. Furthermore, Dma1 is not recruited to the mother vacuole in the *myo2-D1297N* mutant. These observations raise the question of whether phosphorylation of Vac17-Thr240 is bud-specific. Surprisingly, we found that in the *myo2-D1297N* mutant, where Vac17-GFP is localized to the mother vacuole, Vac17-Thr240 was phosphorylated (Figures 5E and 5F). We compared the phosphorylation of Vac17-Thr240 in the *myo2-D1297N* mutant with the phosphorylation of the *vac17-S222A* mutant. The S222A point mutation stabilizes Vac17, but still enables vacuole transport and accumulates in the bud (Figure 5E). Vac17-GFP in the *myo2-D1297N* mutant and *vac17-S222A*-GFP are phosphorylated at Thr240 to similar extents. As expected, the *vac17-T240A*-GFP mutant was not phosphorylated at Thr240 (Figure 5F). These results suggest that Thr240 is phosphorylated in the mother cell. Moreover, phosphorylation of Vac17 does not require Myo2. These observations strongly suggest that Vac17 is phosphorylated on Thr240 in the mother cell prior to the attachment of Myo2 to the vacuole and the initiation of vacuole transport. The failure of Dma1 recruitment to the mother vacuole in the *myo2-D1297N* mutant is not due to a defect in the phosphorylation of Vac17-Thr240. Thus, phosphorylation of Vac17-Thr240 is required but not sufficient for recruiting Dma1 to the vacuole.

Dma1/Dma2 function in the ubiquitylation of Vac17

In *S. pombe*, the E3 ubiquitin ligase activity of Dma1 is required for its function as a spindle checkpoint. *S. Pombe* Dma1-Ile194 is a conserved residue in the RING domain required for Dma1 dependent ubiquitylation *in vitro* and for Dma1 spindle checkpoint function *in vivo* (Johnson and Gould, 2011). This conserved isoleucine is critical for the interaction between E3 ubiquitin ligases with their E2 ubiquitin conjugating enzyme binding partners (Zheng et al., 2000). To determine whether the E3 ubiquitin ligase activity of *S. cerevisiae* Dma1 is required for the termination of vacuole transport, we mutated the Dma1-I329 residue which is homologous with *S. pombe* Dma1-I194.

In contrast to Dma1 and Dma1-GFP, the ubiquitylation-defective mutant, *dma1-I329R*-GFP, failed to target Vac17 for degradation or rescue the termination of vacuole transport in the *dma1*Δ mutant (Figures 6A, S6A and S6B). Moreover, the vacuole accumulates with Vac17-GFP and Myo2-Venus at the mother-bud neck in large budded cells in the *dma1-I329R* mutant (Figures 6B and 6C). Thus, Dma1 dependent ubiquitylation is required for Vac17 degradation and the detachment of the vacuole from Myo2. In *in vitro* binding experiments, we found that GST-*dma1-I329R* bound Vac17-TAP from cell extracts (Figure 6D) which suggests that the E3 ubiquitin ligase activity of Dma1 is not required for Dma1 to bind Vac17.

We found that the levels of the ubiquitylation defective mutant *dma1-I329R*-GFP are higher than wild-type levels (Figure 6A). Wild-type Dma1 auto-ubiquitylates *in vitro* (Loring et al., 2008), which predicts that the *dma1-I329R* mutant is defective in regulating its own turnover. Given that Vac17 recruits Dma1 to the vacuole and that both Vac17 and *dma1-I329R* levels are elevated (Figure 6A) may explain why *dma1-I329R*-GFP localizes to a broader area on the bud vacuole (Figure S6C).

The requirement for the E3 ligase activity of Dma1 for Vac17 degradation suggests that Vac17 is ubiquitylated. Using anti-GFP antibodies, we immunoprecipitated Vac17-GFP from cells expressing myc tagged ubiquitin (myc-Ub). Immunoblot analysis with anti-myc antibodies showed that Vac17-GFP was ubiquitylated *in vivo*. However, in the absence of *DMA1*/*DMA2*, Vac17-GFP levels were elevated but not detectably ubiquitylated (Figure 6E). These results strongly suggest that Vac17 is ubiquitylated *in vivo* in a Dma1/Dma2 dependent manner.

That Vac17 is ubiquitylated suggests that the ubiquitin proteasome system (UPS) is important for Vac17 degradation. We found that Vac17 levels were elevated in the E1 mutant, *uba1-2*, as well as in the proteasome mutants tested, *pre1-1*, *doa3-T76A* and *pup1-K58E*/*pup3-E151K* (Figure 6F). These results suggest that Dma1 ubiquitylates Vac17 and targets Vac17 for degradation via the proteasome.

Discussion

Within a single cell type, myosin V transports multiple organelles. Accurate transport requires that myosin V attaches to cargoes at their original locations and detaches from cargoes at their destinations. Accurate release of organelles from myosin V is critical for

their proper subcellular location (Tang et al., 2003). Our findings suggest that the detachment of cargoes from myosin V occurs in multiple steps along the entire route of cargo transport. Phosphorylation of Vac17-Thr240 occurs in the mother cell and sets up the termination of vacuole transport which occurs later in the bud. Vac17-Thr240 is phosphorylated at the same cellular location where Cdk1 phosphorylates Vac17 at S119, T149, S178, and T248 to recruit Myo2, which initiates vacuole transport (Peng and Weisman, 2008). Because phosphorylation of Vac17-Thr240 does not require Myo2, it is likely that phosphorylation of the 4 Cdk1 sites and Thr240 occur concurrently prior to the initiation of vacuole transport. Moreover, phosphorylation of Thr240 likely does not require Cdk1 phosphorylation of Vac17. In the *vac17-S119/T149/S178/T248A* mutant, vacuoles that are transported to the bud undergo normal release from Myo2 (data not shown).

Our results demonstrate that Thr240 phosphorylation creates a binding site on Vac17 critical for the recruitment of Dma1 to the vacuole. Intriguingly, while phosphorylation of Vac17-Thr240 occurs in the mother cell and does not require the attachment of Myo2 to the vacuole, Dma1 is first observed on the vacuole in the bud and its recruitment to the vacuole requires Myo2. This suggests that either Dma1 recognizes the intact Myo2/Vac17/Vac8 vacuole transport or that Dma1 is recruited to the vacuole in the bud. Furthermore, these results suggest that Thr240 phosphorylation is required but not sufficient for Dma1 recruitment. Moreover, our results suggest that the regulated recruitment of Dma1 to the vacuole is critical for Vac17 degradation.

Notably, after Dma1 is recruited to the vacuole, there is a delay in the mechanism which terminates vacuole transport. Dma1 moves with the vacuole to the bud tip and persists on the vacuole after the bud vacuole separates from the mother vacuole. This suggests that Dma1 activity is regulated so that termination of vacuole transport is coordinated with the resolution of the vacuole segregation structure. Overall, our findings suggest that Dma1 recruitment and function are modulated by at least three events: 1) Vac17 phosphorylation on Thr240, 2) Myo2 attachment to the vacuole and 3) the resolution of the segregation structure.

We further find that Dma1 and Dma2 function in the ubiquitylation of Vac17 *in vivo*. Dma1 dependent ubiquitylation targets Vac17 for degradation via the proteasome which releases the vacuole from Myo2 (Figure 7). In addition to the vacuole, we found that the termination of peroxisome transport also requires *DMA1* and *DMA2* (Figure 1E). Like the vacuole, peroxisomes are transported by Myo2 via a cargo adaptor, Inp2. The mechanisms that detach the vacuole from Myo2 also likely terminate the transport of peroxisomes. Together, these studies suggest that the degradation of cargo adaptors by the Ub-proteasome system may be a common mechanism to release cargoes from molecular motors.

Interestingly, Dma1 is a checkpoint protein which monitors spindle alignment and regulates mitotic exit and cytokinesis. Given that Dma1 regulates multiple cell cycle coordinated events, it is tempting to speculate that Dma1 coordinates the termination of vacuole and peroxisome transport with mitotic exit and cytokinesis.

Myosin V and the mechanisms of myosin V based transport are conserved from yeast to vertebrates. In *S. cerevisiae*, there are 2 class V myosins, Myo2 and Myo4. Mammals have 3 class V myosins, myosin Va, Vb and Vc (Desnos et al., 2007; Hammer and Sellers, 2011; Weisman, 2006). Like Myo2, myosin Va, Vb and Vc move cargoes via cargo specific adaptor proteins. For example, myosin Va transports melanosomes via binding melanophilin and Rab27a (Fukuda et al., 2002; Strom et al., 2002; Wu et al., 2002). Notably, melanophilin contains 3 PEST sequences, which are important for melanophilin turnover and melanosome transport (Fukuda and Itoh, 2004). Intriguingly, western blot analyses show that melanophilin, like Vac17, runs at a higher molecular weight than predicted, suggesting that melanophilin may be phosphorylated (Wu et al., 2002). Given the similarities between Vac17 and melanophilin, we propose that the mechanisms that regulate Vac17 and the termination of vacuole transport may be similar to those that regulate the detachment of other cargoes from myosin V in higher eukaryotes.

Evidence from *Xenopus laevis* suggests that, in addition to cargo adaptors, the cargo binding domain of myosin V may also play a critical role in the detachment of cargoes. In Xenopus, Calcium/calmodulin-dependent protein kinase II (CaMKII) directly phosphorylates the myosin V cargo binding domain (Karcher et al., 2001). This phosphorylation event causes the release of the melanosome from myosin V. Thus, phosphorylation of both myosin V and its cargo adaptor followed by degradation of the cargo adaptor may be common mechanisms that regulate the termination of myosin V transport.

Experimental procedures

Yeast Strains, Plasmids and Media

Yeast cultures were grown in yeast extract peptone dextrose (YEPD) containing 1% yeast extract, 2% peptone and 2% dextrose or synthetic complete (SC) media lacking the indicated amino acid(s) at 24°C unless specified. Yeast strains and plasmids are listed in Tables S1 and S2 respectively (See Supplemental Tables S1 and S2).

Western Blot Analysis

Cells were lysed in 1 ml 0.2 M NaOH/ 0.2% β-mercaptoethanol and 100 μl trichloroacetic acid (TCA) was added. Precipitated proteins were harvested via centrifugation at 12,000 rpm and resuspended in 100 μl 2X SDS sample buffer. 20 μl of 1 M Tris base (pH ~11) was then added, samples were heated at 75°C and analyzed via immunoblot (Peng and Weisman, 2008). For immunoblot analyses, mouse anti-GFP (1:1,000; Roche), rabbit anti-GFP (1:1,000; abcam), rabbit anti-TAP (1:1,000; Thermo Scientific), mouse anti-Pgk1 (1:10,000; Invitrogen), sheep anti-Vac17 (1:1,000) and rabbit anti-phosphoThr240 (1:2,500) antibodies were used.

In vivo ubiquitylation experiments

Cells were co-transformed with pVT102-*VAC17*-GFP and CUP1-myc-Ub plasmids. Myc-Ub expression was induced with 100μM $CuCl_2$. Vac17-GFP was immunoprecipitated as described above and analyzed via immunoblot using anti-myc antibodies (1:2,000; Cell Signaling).

Microscopy

To visualize vacuoles, cells were labeled with 12 μg FM4-64 in 250 μL media for 1 hour, then washed twice and grown in 5 ml fresh media for one doubling time (2-3 hours). Live cell images were obtained on a DeltaVision Restoration system (Applied Precision) using an inverted epifluorescence microscope (IX-71; Olympus) with a charge-coupled device camera (Cool-SNAP HQ; Photometrics) and processed in Photoshop.

Whole Genome Sequencing

Wild-type and mutant backcross pools were derived from sporulation of diploid strain LWY10741, which was obtained by mating strains *vac22-1* and LWY3250 (wild-type). Construction of pooled libraries and analysis of the resulting Illumina sequencing data was performed as previously described (Birkeland et al., 2010). The filter for potential *vac22-1* mutations demanded that (i) the candidate mutation changed the coding of a yeast ORF, (ii) the mutation site was covered by at least three reads in both the wild-type and *vac22-1* mutant pools, (iii) all reads in the wild-type pool corresponded to the wild-type allele, and (iv) all reads in the mutant pool corresponded to the mutant allele. This filter yielded only the *dma1-G232R* mutation. We note that the *vac22-1* mutant pool was a low quality library with only 4-fold base coverage of the yeast genome. As a result, we cannot rule out that other potential candidate mutations were missed. However, based on the biological analysis of *dma1-G232R* it is likely to be the sole cause of the *vac22-1* phenotype.

In vitro binding experiments

In vitro binding experiments were performed using recombinant GST tagged fusion proteins expressed in BL21 star DE3 cells and yeast cell extracts. For expression of GST fusion proteins see (Loring et al., 2008) and Supplemental Experimental Procedures.

Thermostability Measurements

GST and GST-Dma1 samples were prepared in 50 mM Tris-HCl, pH 7.5, 150 mM NaCl, 0.01% Triton X-100, 5 mM β-mercaptoethanol, 100 mM ANS and overlaid with silicone oil. Measurements were taken using a Thermofluor 384-well plate reader (Johnson & Johnson). See Supplemental Experimental Procedures.

EMS Mutagenesis

Wild-type (LWY3250) cells transformed with pRS416-*VAC17-GFP* were grown in SCUra + 0.5% CA media. Cells were resuspended in 1 ml 0.1 M sodium phosphate buffer, pH 7.0. EMS (Sigma) was added to a final concentration of 36.18 mg/ml and cells were incubated at 24 °C for 1 hour. Cells were washed with ddH_20, then washed twice with 5% sodium thiosulfate and were grown in SC-Ura+ 0.5% CA media for 12 hours. Mutants with elevated Vac17-GFP fluorescence were isolated via Fluorescence Activated Cell Sorting (FACS) and were plated on SC-Ura media. Microscopy and western blot analysis were used to confirm the elevation of Vac17 levels in these mutants.

Supplementary Material

Refer to Web version on PubMed Central for supplementary material.

Acknowledgments

We thank Dr. John Tesmer and Dr. Kristoff Homan (U. of Michigan) for their help with the Thermofluor assay. We thank Dr. Mark Hochstrasser (Yale) for providing the E1 and proteasome mutants strains. We thank Dr. Yui Jin (U. of Michigan) for the mCherry-*MYO2* plasmid and Dr. Robert Piper (U. of Iowa) for the CUP1-myc-Ub plasmid. We thank Melehia Frauenholtz for contributing to the screen that identified *DMA1*. This work was supported by National Institutes of Health grant R37- GM062261 to L.S. Weisman. R.R. Valiathan was supported in part through American Heart Association postdoctoral fellowship AHA Award 0825819G. R.G. Yau was supported in part through National Institutes of Health grant T32-GM007315.

References

Bartholomew CR, Hardy CF. p21-activated kinases Cla4 and Ste20 regulate vacuole inheritance in Saccharomyces cerevisiae. Eukaryotic cell. 2009; 8:560–572. [PubMed: 19218422]

Bieganowski P, Shilinski K, Tsichlis PN, Brenner C. Cdc123 and checkpoint forkhead associated with RING proteins control the cell cycle by controlling eIF2gamma abundance. The Journal of biological chemistry. 2004; 279:44656–44666. [PubMed: 15319434]

Birkeland SR, Jin N, Ozdemir AC, Lyons RH Jr. Weisman LS, Wilson TE. Discovery of mutations in Saccharomyces cerevisiae by pooled linkage analysis and whole-genome sequencing. Genetics. 2010; 186:1127–1137. [PubMed: 20923977]

Desnos C, Huet S, Darchen F. 'Should I stay or should I go?': myosin V function in organelle trafficking. Biology of the cell / under the auspices of the European Cell Biology Organization. 2007; 99:411–423. [PubMed: 17635110]

Durocher D, Henckel J, Fersht AR, Jackson SP. The FHA domain is a modular phosphopeptide recognition motif. Molecular cell. 1999; 4:387–394. [PubMed: 10518219]

Durocher D, Taylor IA, Sarbassova D, Haire LF, Westcott SL, Jackson SP, Smerdon SJ, Yaffe MB. The molecular basis of FHA domain:phosphopeptide binding specificity and implications for phospho-dependent signaling mechanisms. Molecular cell. 2000; 6:1169–1182. [PubMed: 11106755]

Eves PT, Jin Y, Brunner M, Weisman LS. Overlap of cargo binding sites on myosin V coordinates the inheritance of diverse cargoes. The Journal of cell biology. 2012; 198:69–85. [PubMed: 22753895]

Fagarasanu A, Fagarasanu M, Eitzen GA, Aitchison JD, Rachubinski RA. The peroxisomal membrane protein Inp2p is the peroxisome-specific receptor for the myosin V motor Myo2p of Saccharomyces cerevisiae. Developmental cell. 2006; 10:587–600. [PubMed: 16678774]

Fortsch J, Hummel E, Krist M, Westermann B. The myosin-related motor protein Myo2 is an essential mediator of bud-directed mitochondrial movement in yeast. The Journal of cell biology. 2011; 194:473–488. [PubMed: 21807878]

Fraschini R, Bilotta D, Lucchini G, Piatti S. Functional characterization of Dma1 and Dma2, the budding yeast homologues of Schizosaccharomyces pombe Dma1 and human Chfr. Molecular biology of the cell. 2004; 15:3796–3810. [PubMed: 15146058]

Fukuda M, Itoh T. Slac2-a/melanophilin contains multiple PEST-like sequences that are highly sensitive to proteolysis. The Journal of biological chemistry. 2004; 279:22314–22321. [PubMed: 15145961]

Fukuda M, Kuroda TS, Mikoshiba K. Slac2-a/melanophilin, the missing link between Rab27 and myosin Va: implications of a tripartite protein complex for melanosome transport. The Journal of biological chemistry. 2002; 277:12432–12436. [PubMed: 11856727]

Ghaemmaghami S, Huh WK, Bower K, Howson RW, Belle A, Dephoure N, O'Shea EK, Weissman JS. Global analysis of protein expression in yeast. Nature. 2003; 425:737–741. [PubMed: 14562106]

Guertin DA, Venkatram S, Gould KL, McCollum D. Dma1 prevents mitotic exit and cytokinesis by inhibiting the septation initiation network (SIN). Developmental cell. 2002; 3:779–790. [PubMed: 12479804]

Hammer JA 3rd, Sellers JR. Walking to work: roles for class V myosins as cargo transporters. Nature reviews. 2011; 13:13–26.

Ishikawa K, Catlett NL, Novak JL, Tang F, Nau JJ, Weisman LS. Identification of an organelle-specific myosin V receptor. The Journal of cell biology. 2003; 160:887–897. [PubMed: 12642614]

Itoh T, Toh EA, Matsui Y. Mmr1p is a mitochondrial factor for Myo2p-dependent inheritance of mitochondria in the budding yeast. The EMBO journal. 2004; 23:2520–2530. [PubMed: 15201867]

Itoh T, Watabe A, Toh EA, Matsui Y. Complex formation with Ypt11p, a rab-type small GTPase, is essential to facilitate the function of Myo2p, a class V myosin, in mitochondrial distribution in Saccharomyces cerevisiae. Molecular and cellular biology. 2002; 22:7744–7757. [PubMed: 12391144]

Jin Y, Sultana A, Gandhi P, Franklin E, Hamamoto S, Khan AR, Munson M, Schekman R, Weisman LS. Myosin V transports secretory vesicles via a Rab GTPase cascade and interaction with the exocyst complex. Developmental cell. 2011; 21:1156–1170. [PubMed: 22172676]

Johnson AE, Gould KL. Dma1 ubiquitinates the SIN scaffold, Sid4, to impede the mitotic localization of Plo1 kinase. The EMBO journal. 2011; 30:341–354. [PubMed: 21131906]

Karcher RL, Roland JT, Zappacosta F, Huddleston MJ, Annan RS, Carr SA, Gelfand VI. Cell cycle regulation of myosin-V by calcium/calmodulin-dependent protein kinase II. Science (New York, NY. 2001; 293:1317–1320.

Karpova TS, Reck-Peterson SL, Elkind NB, Mooseker MS, Novick PJ, Cooper JA. Role of actin and Myo2p in polarized secretion and growth of Saccharomyces cerevisiae. Molecular biology of the cell. 2000; 11:1727–1737. [PubMed: 10793147]

Korinek WS, Copeland MJ, Chaudhuri A, Chant J. Molecular linkage underlying microtubule orientation toward cortical sites in yeast. Science (New York, NY. 2000; 287:2257–2259.

Lillie SH, Brown SS. Immunofluorescence localization of the unconventional myosin, Myo2p, and the putative kinesin-related protein, Smy1p, to the same regions of polarized growth in Saccharomyces cerevisiae. The Journal of cell biology. 1994; 125:825–842. [PubMed: 8188749]

Lipatova Z, Tokarev AA, Jin Y, Mulholland J, Weisman LS, Segev N. Direct interaction between a myosin V motor and the Rab GTPases Ypt31/32 is required for polarized secretion. Molecular biology of the cell. 2008; 19:4177–4187. [PubMed: 18653471]

Loring GL, Christensen KC, Gerber SA, Brenner C. Yeast Chfr homologs retard cell cycle at G1 and G2/M via Ubc4 and Ubc13/Mms2-dependent ubiquitination. Cell cycle (Georgetown, Tex. 2008; 7:96–105.

Marchal C, Haguenauer-Tsapis R, Urban-Grimal D. A PEST-like sequence mediates phosphorylation and efficient ubiquitination of yeast uracil permease. Molecular and cellular biology. 1998; 18:314–321. [PubMed: 9418878]

Martinez LO, Agerholm-Larsen B, Wang N, Chen W, Tall AR. Phosphorylation of a pest sequence in ABCA1 promotes calpain degradation and is reversed by ApoA-I. The Journal of biological chemistry. 2003; 278:37368–37374. [PubMed: 12869555]

Murone M, Simanis V. The fission yeast dma1 gene is a component of the spindle assembly checkpoint, required to prevent septum formation and premature exit from mitosis if spindle function is compromised. The EMBO journal. 1996; 15:6605–6616. [PubMed: 8978687]

Peng Y, Weisman LS. The cyclin-dependent kinase Cdk1 directly regulates vacuole inheritance. Developmental cell. 2008; 15:478–485. [PubMed: 18804442]

Pennell S, Westcott S, Ortiz-Lombardia M, Patel D, Li J, Nott TJ, Mohammed D, Buxton RS, Yaffe MB, Verma C, et al. Structural and functional analysis of phosphothreonine-dependent FHA domain interactions. Structure. 2010; 18:1587–1595. [PubMed: 21134638]

Pruyne D, Legesse-Miller A, Gao L, Dong Y, Bretscher A. Mechanisms of polarized growth and organelle segregation in yeast. Annual review of cell and developmental biology. 2004; 20:559–591.

Santiago-Tirado FH, Legesse-Miller A, Schott D, Bretscher A. PI4P and Rab inputs collaborate in myosin-V-dependent transport of secretory compartments in yeast. Developmental cell. 2011; 20:47–59. [PubMed: 21238924]

Strom M, Hume AN, Tarafder AK, Barkagianni E, Seabra MC. A family of Rab27-binding proteins. Melanophilin links Rab27a and myosin Va function in melanosome transport. The Journal of biological chemistry. 2002; 277:25423–25430. [PubMed: 11980908]

Tang F, Kauffman EJ, Novak JL, Nau JJ, Catlett NL, Weisman LS. Regulated degradation of a class V myosin receptor directs movement of the yeast vacuole. Nature. 2003; 422:87–92. [PubMed: 12594460]

Tang F, Peng Y, Nau JJ, Kauffman EJ, Weisman LS. Vac8p, an armadillo repeat protein, coordinates vacuole inheritance with multiple vacuolar processes. Traffic (Copenhagen, Denmark). 2006; 7:1368–1377.

Weisman LS. Organelles on the move: insights from yeast vacuole inheritance. Nature reviews. 2006; 7:243–252.

Weisman LS, Wickner W. Intervacuole exchange in the yeast zygote: a new pathway in organelle communication. Science (New York, NY. 1988; 241:589–591.

Wu XS, Rao K, Zhang H, Wang F, Sellers JR, Matesic LE, Copeland NG, Jenkins NA, Hammer JA 3rd. Identification of an organelle receptor for myosin-Va. Nature cell biology. 2002; 4:271–278.

Zheng N, Wang P, Jeffrey PD, Pavletich NP. Structure of a c-Cbl-UbcH7 complex: RING domain function in ubiquitin-protein ligases. Cell. 2000; 102:533–539. [PubMed: 10966114]

Highlights

- Release from Myo2 is critical for the localization of vacuoles and peroxisomes
- Dma1, an E3 ligase, is required for the regulated release of Myo2 from its cargoes
- Phosphorylation of the Myo2 cargo adaptor, Vac17, recruits Dma1 to the vacuole
- Dma1 terminates vacuole transport via targeting Vac17 for proteasomal degradation

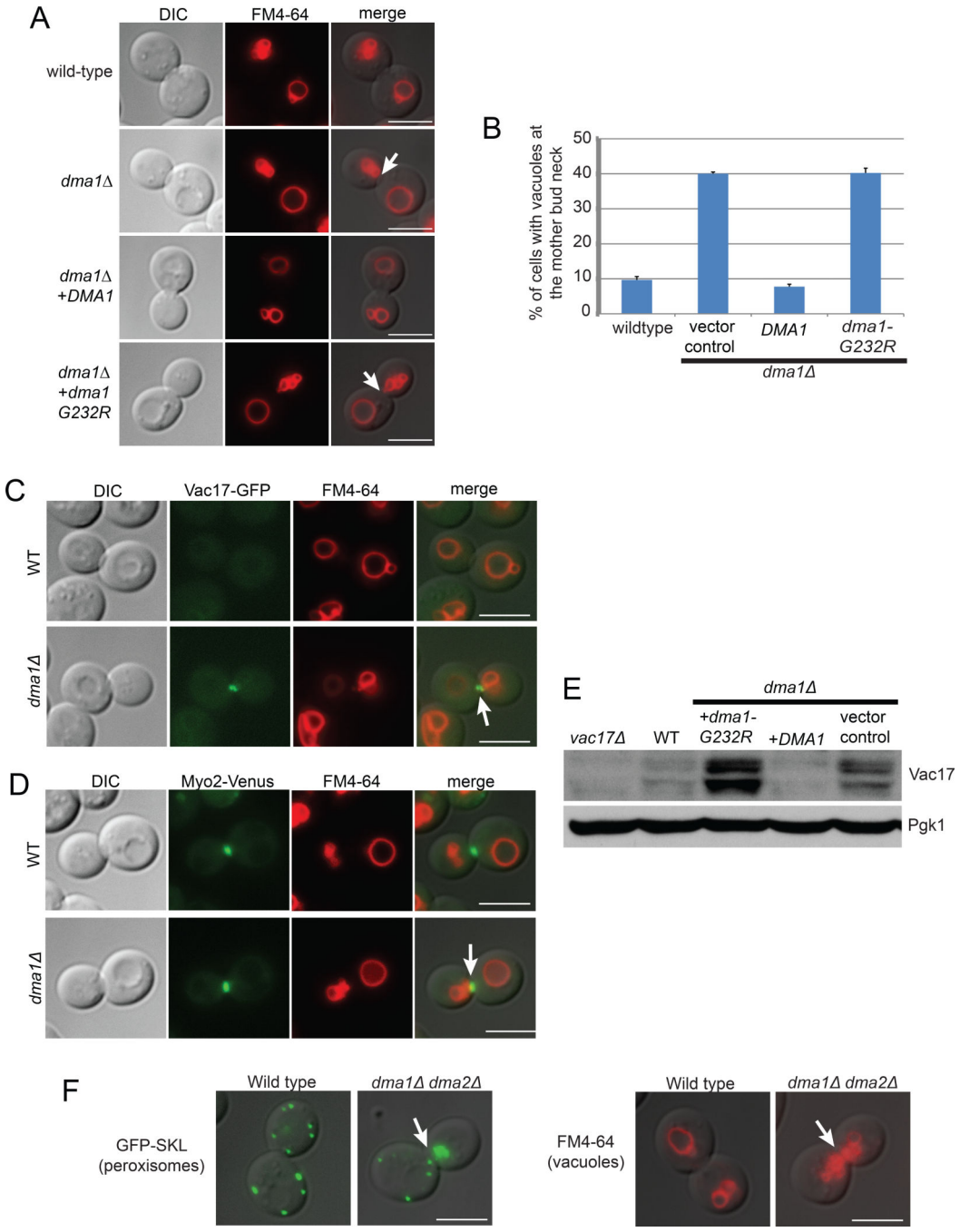

Figure 1. *DMA1* is required for the termination of Myo2 dependent transport

(A) The vacuole accumulates at the mother-bud neck in the *dma1*Δ mutant (arrows), expression of *DMA1* but not *dma1-G232R* restores the proper position of the vacuole in the bud. (B) Percentage of large budded cells with the accumulation of vacuoles at the mother-bud neck in the absence of *DMA1*. Expression of *DMA1* but not *dma1-G232R* restores the proper position of the bud vacuole in the *dma1*Δ mutant. Error bars; standard error of the mean (SEM). A minimum of 100 cells were counted per experiment for 3 experiments. (C) Vac17-GFP and vacuoles are mis-targeted to the mother-bud neck in the *dma1*Δ mutant. (D) The vacuole colocalizes with Myo2-Venus at the mother-bud neck in the *dma1*Δ mutant. (E) Vac17 levels are elevated in the *dma1*Δ mutant, expression of *DMA1* but not *dma1-G232R* rescues Vac17 levels. (F) Both peroxisomes (GFP-SKL) and

vacuoles (FM4-64) are mis-targeted to the mother-bud neck in large budded cells in the *dma1*Δ *dma2*Δ mutant. Bar = 5 μm. See also Figure S1.

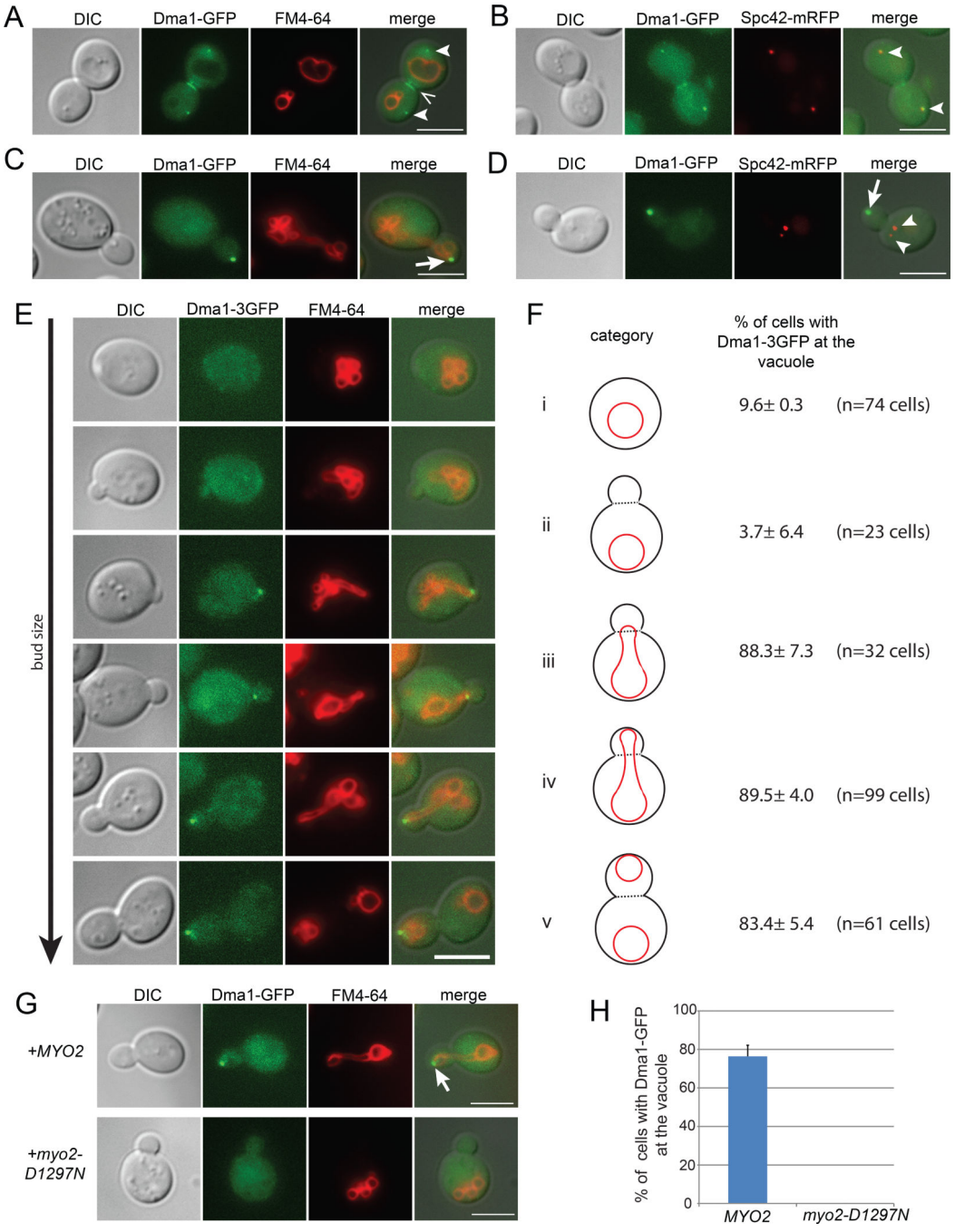

Figure 2. Dma1 localizes to the SPBs, septin ring and the vacuole

(A) In large budded cells, Dma1-GFP localizes to regions consistent with the SPBs (arrowheads) and septin ring (<), and (B) colocalizes with Spc42-mRFP, a component of the SPB (arrow heads). (C) In small budded cells, Dma1-GFP localizes to the vacuole in the bud (arrow) and (D) does not colocalize with Spc42-mRFP (arrow heads). (E) Dma1-3xGFP is first observed on the vacuole as the vacuole crosses the mother-bud neck. Dma1 remains on the vacuole at the bud tip until after the resolution of the segregation structure. (F) Percentage of cells with Dma1 at the vacuole in (i) unbudded cells, (ii) small budded cells where the vacuole is in the mother, (iii) small budded cells where the vacuole has crossed the mother-bud neck, (iv) small budded cells where the vacuole has reached the bud tip, (v) medium budded cells where the segregation structure was resolved. (G-H) The

*myo2*Δ *dma1*Δ double mutant co-expressing *DMA1*-GFP with *MYO2* or *myo2-D1297N*. (G) Dma1-GFP localizes to the vacuole in the bud in cells expressing *MYO2*, but fails to localize to the mother vacuole in cells expressing *myo2-D1297N*, a mutant defective in vacuole transport. (H) Quantification of the percentage of small budded cells where Dma1-GFP localizes to the vacuole. Z-sections of small budded cells were analyzed. A minimum of 25 cells were counted per experiment for 3 experiments. Error bars; standard error of the mean (SEM). Bar = 5 μm. See also Figure S2.

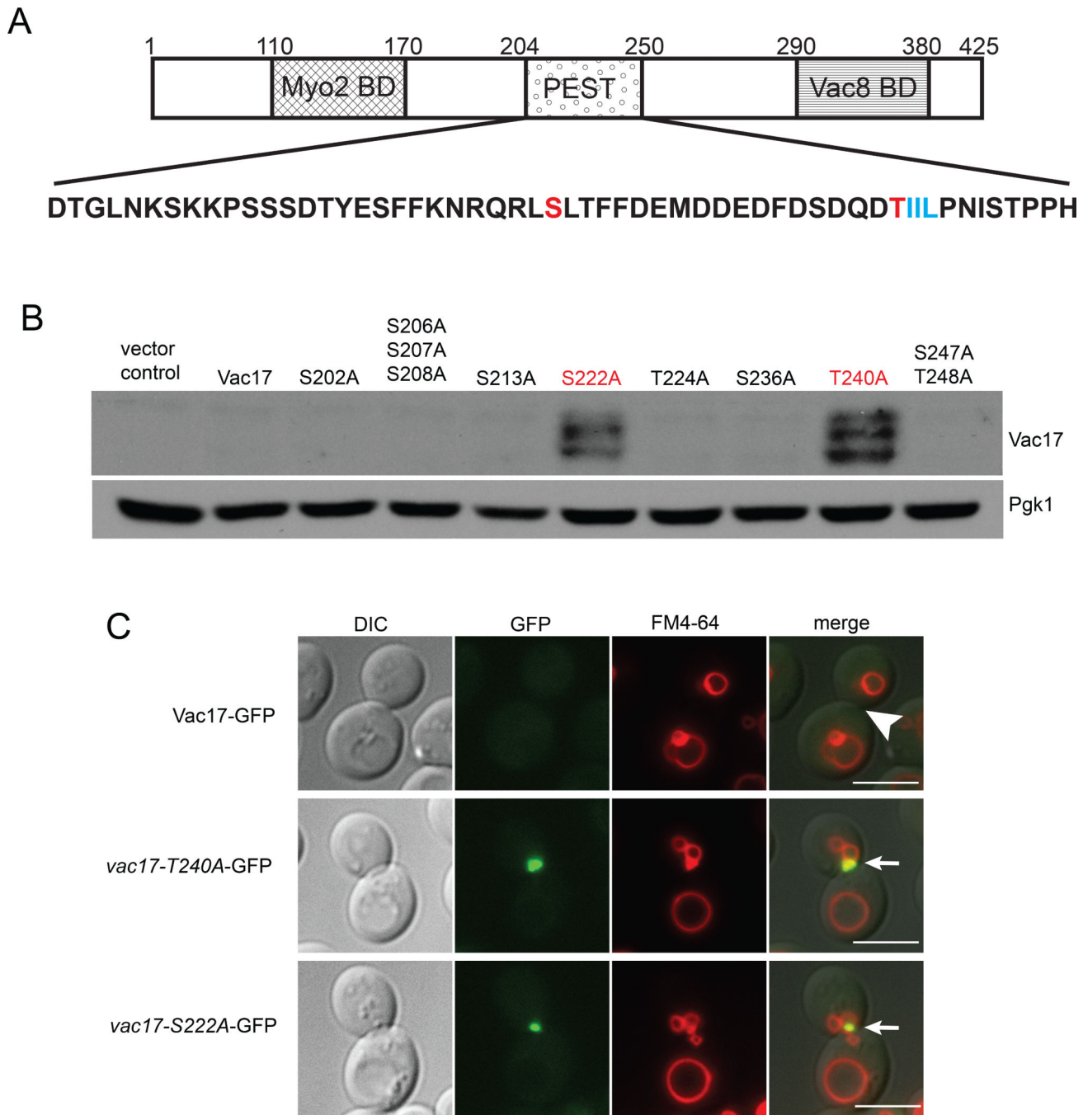

Figure 3. Identification of Vac17 residues required for the termination of vacuole movement and Vac17 turnover

(A) Vac17 residues 204-250 comprise the PEST sequence (Tang et al., 2003). Red; potential phosphorylation sites required for Vac17 turnover. Blue; FHA binding motif. (B) Western blot analysis of *vac17* point mutants from an alanine scan of all the serine and threonine residues within the Vac17 PEST sequence. anti-Vac17 antibodies; 1:1,000 dilution. (C) *vac17-T240A*-GFP and *vac17-S222A*-GFP as well as vacuoles are mis-targeted to the mother bud neck (arrows). Bar = 5 μm. See also Figure S3.

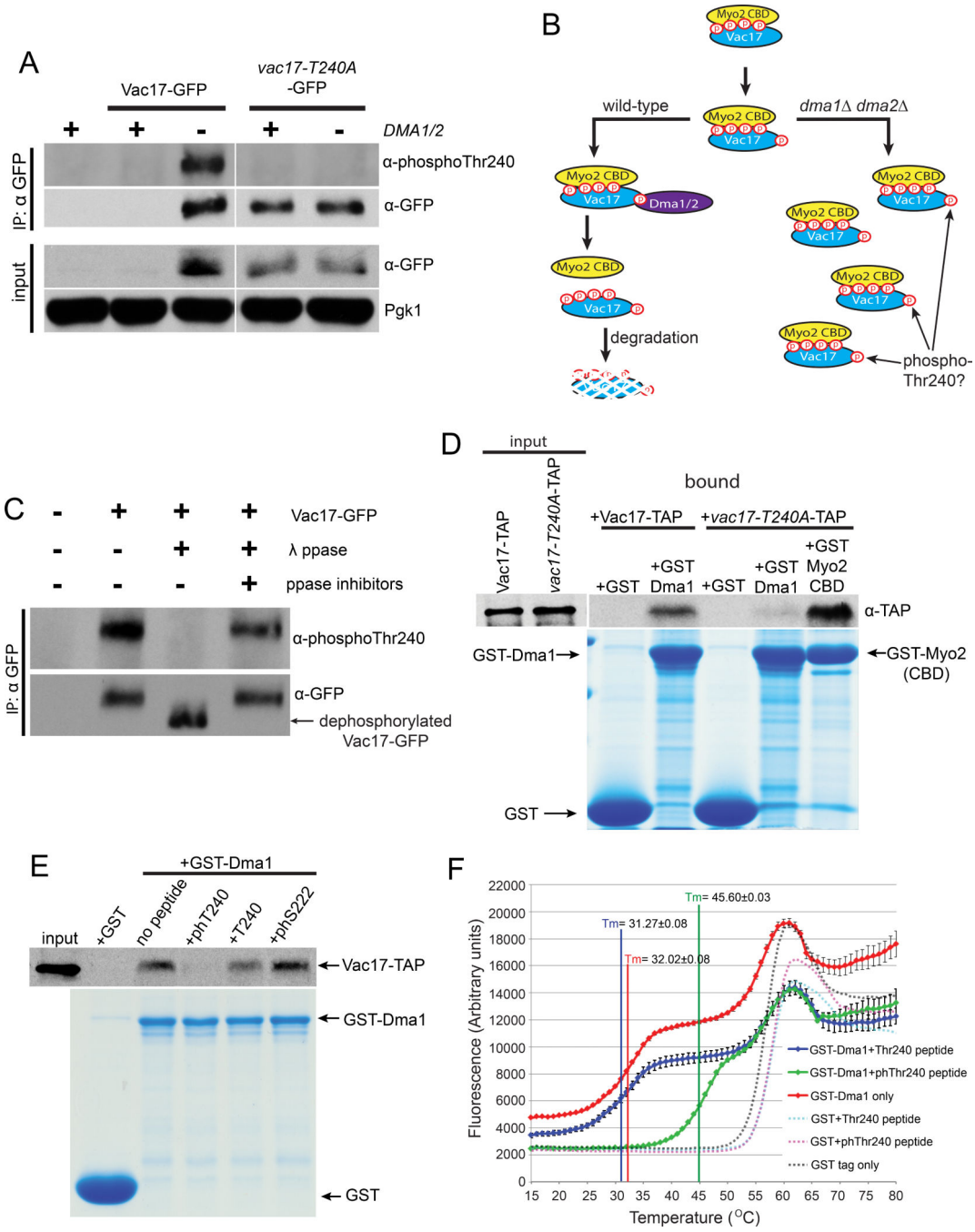

Figure 4. Dma1 binds directly to phosphorylated Vac17-Thr240 *in vitro*

(A) In the *dma1*Δ *dma2*Δ mutant, Vac17-GFP is stabilized (input). *vac17-T240A*-GFP levels are higher than Vac17-GFP and are not affected by the deletion of *DMA1*/*DMA2*. Vac17-GFP was immunoprecipitated with anti-GFP antibodies and analyzed using antibodies generated against a peptide with a phosphorylated Thr240 (anti-phosphoThr240). These antibodies recognize Vac17-GFP but not *vac17-T240A*-GFP. (B) Model illustrating the hypothesis that in wild-type cells, Dma1 and Dma2 target phosphorylated Vac17 for degradation. This model predicts that phosphorylated Vac17 would accumulate in a *dma1*Δ *dma2*Δ mutant. (C) λ-phosphatase (ppase) dephosphorylates Vac17-GFP as indicated by an increase in electrophoretic mobility (arrow). Inhibition of λ-ppase activity blocks dephosphorylation. The anti-phosphoThr240 antibody does not recognize

dephosphorylated Vac17-GFP. (D) Immobilized recombinant GST-Dma1 binds Vac17-TAP but not *vac17-T240A*-TAP from cell lysates. GST-Myo2 cargo binding domain binds *vac17-T240A*-TAP which strongly suggests that *vac17-T240A* folds properly. (E) In a competition experiment, the phospho-Thr240 peptide blocked GSTDma1 from binding Vac17-TAP whereas a peptide with an unphosphorylated Thr240 or phospho-Ser222 did not block binding. anti-phosphoThr240 antibodies; 1:2,500 dilution. anti-GFP antibodies; 1:1,000 dilution. anti-TAP antibodies; 1:1,000 dilution. Staining; Gelcode Blue stain reagent (Thermo scientific). (F) ThermoFluor was used to test the thermostability of GST and GST-Dma1. Heat induced protein unfolding was measured as an increase in ANS fluorescence. The T_m of GST-Dma1 alone (red solid line), with an unphosphorylated peptide (blue solid line) or a phospho-Thr240 peptide were 32.02±0.08 °C, 31.27±0.08 °C and 45.60±0.03 °C respectively. The T_m of the GST tag alone (black dotted line), with an unphosphorylated peptide (turquoise dotted line) or a phospho-Thr240 peptide (pink dotted line) were 56.24±0.06 °C, 57.40±0.01 °C and 57.22±0.05 °C respectively. Error bars; standard error of the mean (SEM). See also Figure S4.

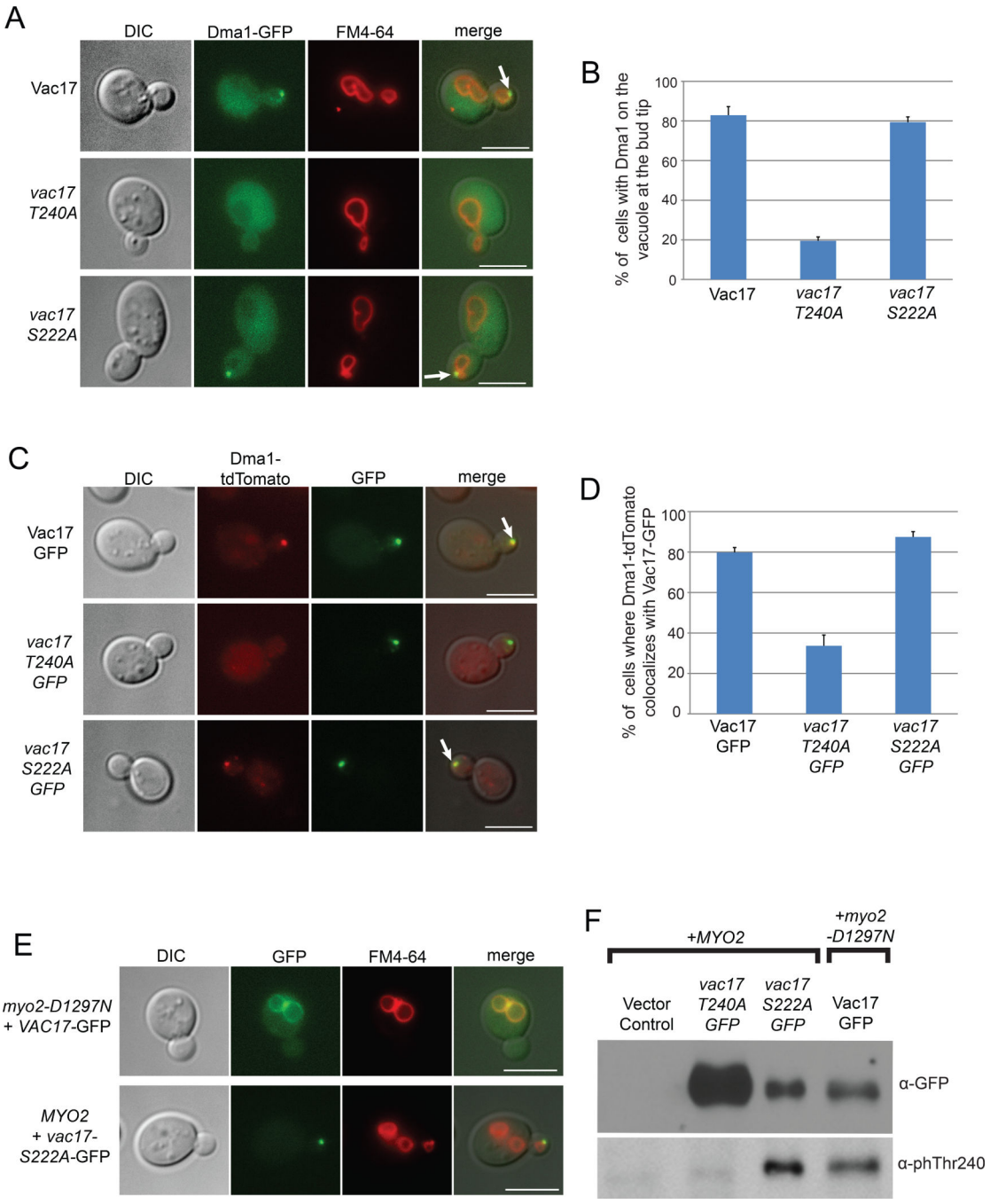

Figure 5. Dma1 recruitment to the Myo2/Vac17 vacuole transport complex requires the interaction between Dma1 and Vac17

(A) Dma1-GFP localizes to the vacuole at the bud tip (arrows) in cells expressing *VAC17* and *vac17-S222A* but not *vac17-T240A*. (B) Quantification of the percentage of small budded cells where Dma1-GFP is localized to the bud vacuole. A minimum of 30 cells were counted per experiment for 3 experiments. (C) Dma1-tdTomato colocalizes with Vac17-GFP and *vac17-S222A*-GFP but not with *vac17-T240A*-GFP. Colocalization occurs at the bud tip (arrows). (D) Quantification of the percentage of small budded cells where Dma1-tdTomato colocalizes with GFP tagged Vac17 and *vac17* point mutants. A minimum of 13 cells were counted per experiment for 3 experiments. (E-F) In a *myo2*Δ *vac17*Δ double mutant, *myo2-D1297N* and *VAC17*-GFP or *MYO2* and *vac17-S222A*-GFP were co-expressed from plasmids. (E) In cells expressing *myo2-D1297N*,

Vac17-GFP is localized throughout the mother vacuole. In cells expressing *MYO2*, *vac17-S222A*-GFP and the vacuole are transported to the bud. (F) Vac17-GFP in the *myo2-D1297N* mutant and *vac17-S222A*-GFP in cells expressing *MYO2* are phosphorylated at Thr240 to a similar extent. anti-phosphoThr240 antibodies; 1:2,500 dilution. anti-GFP antibodies; 1:1,000 dilution. Error bars; SEM. Bar = 5 μm. See also Figure S5.

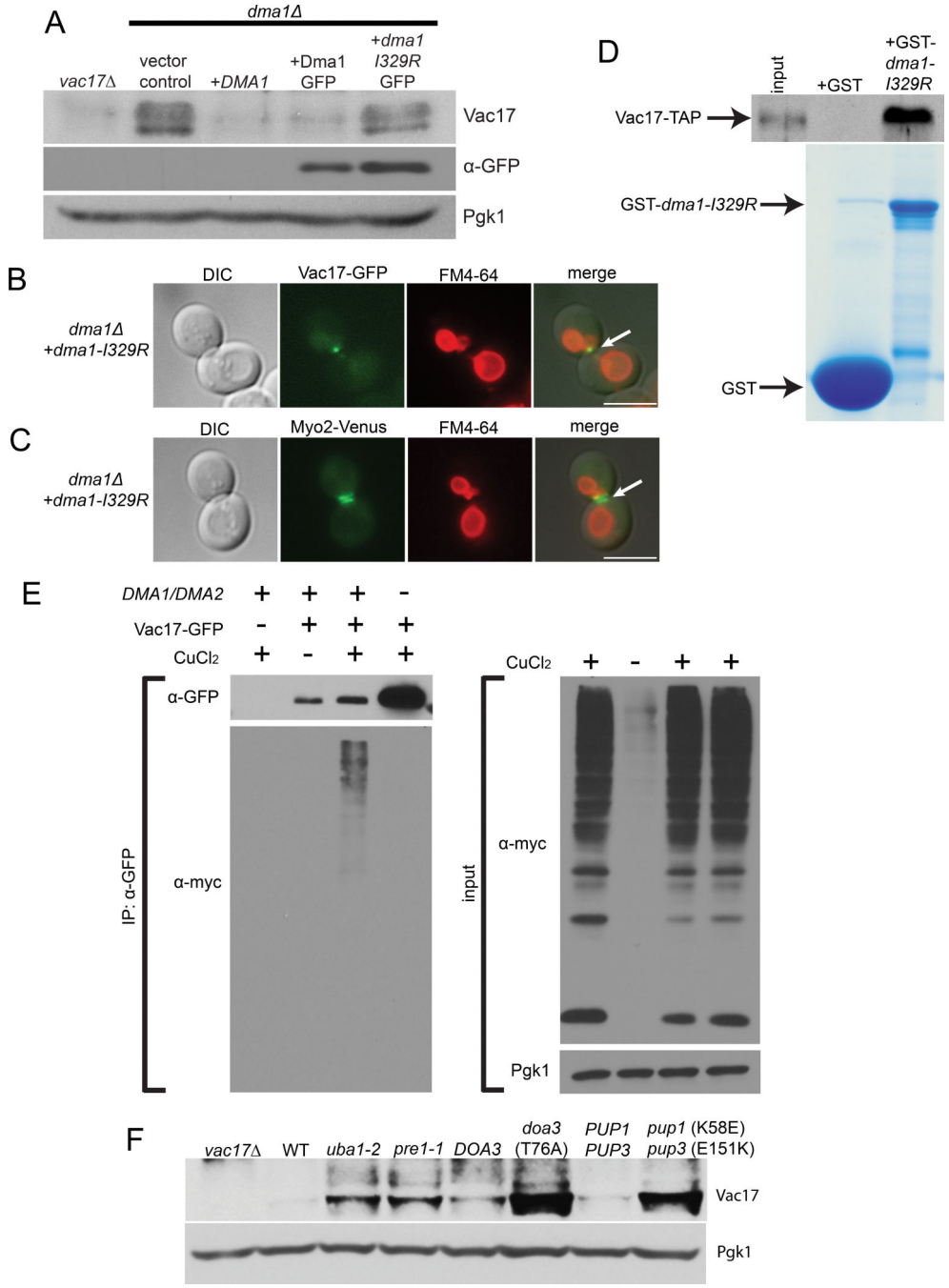

Figure 6. Dma1 dependent ubiquitylation is required for Vac17 turnover and the termination of vacuole movement

(A) Expression of *DMA1* and *DMA1-GFP* but not *dma1-I329R-GFP* rescues Vac17 levels in the *dma1*Δ mutant. (B) Recombinant GST-*dma1-I329R* binds Vac17-TAP in yeast cell lysates. (C-D) In the *dma1-I329R* mutant, Vac17-GFP, the vacuole and Myo2-Venus accumulate at the mother-bud neck of large budded cells. (E) Vac17-GFP is ubiquitylated *in vivo*. Dma1 and Dma2 are required for Vac17-GFP ubiquitylation. (F) Vac17 levels are elevated in the *uba1-2* E1 mutant and in proteasome mutants. anti-GFP antibodies; 1:1,000 dilution. anti-Vac17 antibodies; 1:1000 dilution. anti-TAP antibodies; 1:1,000 dilution. anti-myc antibodies; 1:2,000 dilution. Bar = 5 μm. See also Figure S6.

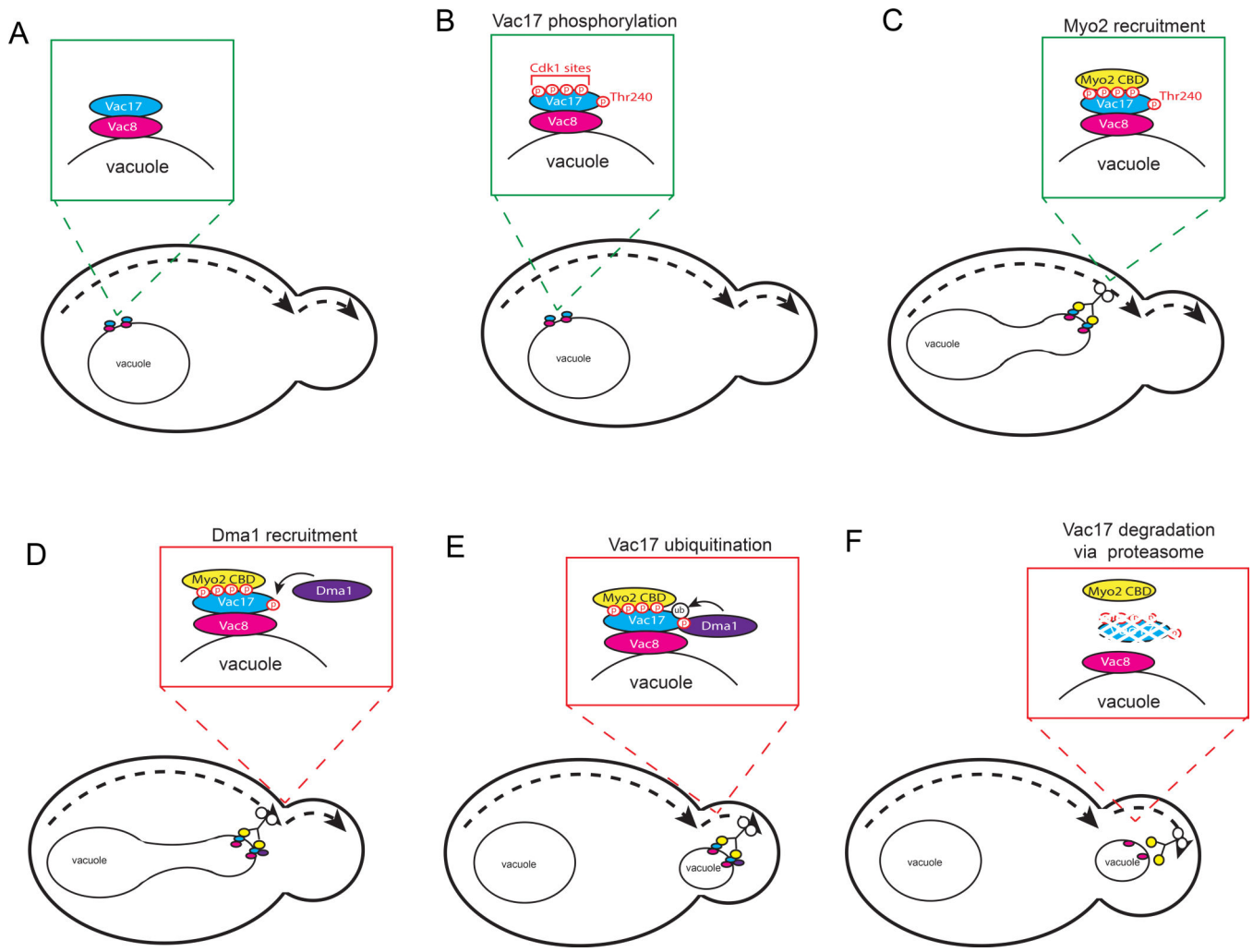

Figure 7. Model for the regulation of vacuole transport

(A-B) Vac17 is phosphorylated at Thr240 as well as 4 Cdk1 sites. (C) Myo2 binds Vac17 and attaches to the vacuole in the mother cell to initiate transport. (D) After assembly of the Myo2/Vac17/Vac8 transport complex, Dma1 is recruited to the vacuole via binding directly to Vac17 at phospho-Thr240. (E-F) After resolution of the segregation structure which separates the bud and mother vacuoles, Dma1 ubiquitylates Vac17 and targets Vac17 for degradation via the proteasome which detaches the vacuole from Myo2 and terminates vacuole transport.